HHS Public Access

Author manuscript

Prostate. Author manuscript; available in PMC 2018 August 01.

Published in final edited form as:

Prostate. 2017 August ; 77(11): 1187–1198. doi:10.1002/pros.23377.

Characterization of a novel p110β-specific inhibitor BL140 that overcomes MDV3100-resistance in castration-resistant prostate cancer cells

Chenchen He[1,2], **Shaofeng Duan**[3], **Liang Dong**[2], **Yifen Wang**[2,#], **Qingting Hu**[2], **Chunjing Liu**[4], **M. Laird Forrest**[4], **Jeffrey M. Holzbeierlein**[2], **Suxia Han**[1,*], and **Benyi Li**[1,2,3,*]

[1]Department of Medical Oncology, The First Affiliated Hospital, Xi'An Jiaotong University School of Medicine, Xi'An 710061, China

[2]Department of Urology, The University of Kansas Medical Center, Kansas City, KS 66160

[3]Pharmaceutical College, Henan University, Kaifeng 475004, China

[4]Department of Pharmaceutical Chemistry, The University of Kansas School of Pharmacy, Lawrence, KS 66045

Abstract

Background—Our previous studies demonstrated that the class IA PI3K/p110β is critical in castration-resistant progression of prostate cancer (CRPC) and that targeting prostate cancer with nanomicelle-loaded p110β-specific inhibitor TGX221 blocked xenograft tumor growth in nude mice, confirming the feasibility of p110β-targeted therapy for CRPCs. To improve TGX221's aqueous solubility, in this study, we characterized four recently synthesized TGX221 analogs.

Methods—TGX221 analog efficacy were examined in multiple prostate cancer cell lines with the SRB cell growth assay, Western blot assay for AKT phosphorylation and cell cycle protein levels. Target engagement with PI3K isoforms was evaluated with cellular thermal shift assay. PI3K activity was determined with the Kinase-Glo Plus luminescent kinase assay. Cell cycle distribution was evaluated with flow cytometry after propidium iodide staining.

Results—As expected, replacing either one of two major functional groups in TGX221 by more hydrophilic groups dramatically improved the aqueous solubility (about 40-fold) compared to TGX221. In the CETSA assay, all the analogs dramatically shifted the melting curve of p110β protein while none of them largely affected the melting curves of p110α, p110γ or Akt proteins, indicating target-specific engagement of these analogs with p110β protein. However, functional evaluation showed that only one of the analogs BL140 ubiquitously inhibited AKT phosphorylation in all CRPC cell lines tested with diverse genetic abnormalities including AR, PTEN and p53 status. BL140 was superior than GSK2636771 (IC_{50} 5.74 *vs* 20.49 nM), the only

*Corresponding authors: Benyi Li, MD/PhD, KUMC Urology, 3901 Rainbow Blvd, Kansas City, KS 66160. bli@kumc.edu. Tell: +19135884773. Suxia Han, MD/PhD, 277 West Yanta Rd, The First Affiliated Hospital, Xi'An Jiaotong University, Xi'An 710061, China. shan87@xjtu.edu.cn. Tell: +8613991822099.

#**Current Address:** State Key Laboratory of Plant Chemistry and Sustainable Utilization of Plant Resources in Western China, Kunmin 650201, China.

Disclosure Statement: None

p110β-selective inhibitor currently in clinical trials, as revealed in an *in vitro* Kinase-Glo assay. Furthermore, BL140 exhibited a stronger inhibitory effect than GSK2636771 on multiple CRPC cell lines including a MDV3100-resistant C4-2B cell subline, indicating BL140 elimination of MDV3100 resistance. Mechanistic studies revealed that BL140 blocked G_1 phase cell cycle entry by reducing cyclin D1 but increasing $p27^{kip1}$ protein levels.

Conclusion—These studies suggested that BL140 is a promising p110β-specific inhibitor with multiple superb properties than GSK2636771 worthy for further clinical development.

Keywords

PI3K; p110β; Enzalutamide; prostate cancer

Introduction

Prostate cancers in the castration-resistant stage (CRPC) are life-threatening as they are not curable in clinic (1). Despite the development of novel androgen receptor antagonist CYP17 inhibitor Abiraterone, Enzalutamide or new immunotherapies, patient survival was only prolonged for a few months in advanced prostate cancers (2–4). Therefore, novel therapy is urgently needed for advanced prostate cancers.

Phosphatidylinositol 3-kinases (PI3Ks) are major cellular signaling molecules that regulate multiple cellular functions (5). The class I PI3Ks have two subtypes, IA p110α/β/δ and IB p110γ. PI3K class IA p110α and p110β are ubiquitously expressed, but there is a functional diversity between these two isoforms (6). The p110β has a distinct role different from p110α in cell survival, DNA replication, cell mitosis, and male fertility while the p110α is mostly associated with insulin or growth factor pathways (7,8). Due to the inactivating mutation of PI3K negative regulator *PTEN* gene (phosphatase and tensin homologue deleted on chromosome 10) or gain-of-function mutations on PI3K isoform genes, elevated PI3K activity has been proposed as one of the major mechanisms for many types of human cancers including prostate cancers (9,10). Meanwhile, recent genomic analysis and deep sequencing data revealed that genetic abnormalities in PTEN/PI3K-AKT were found in up to 40–70% of patients (5,11). Most interestingly, a novel fusion gene with an androgen-regulated prostate-specific acid phosphatase (ACPP) at the 5′ (exon 1–2) fused to *PIK3CB* gene was found in a castration-resistant prostate cancer patient (12), representing one potential mechanism of *PIK3CB* gene upregulation as reported in our publication (13). In addition, current anti-androgen therapies were found to cause elevated PI3K/AKT activation due to compensatory mechanism, indicating combinational inhibition of both PI3K/AKT pathway and androgen receptor has much more advantage compared to single therapy (14–18). In our previous studies, we demonstrated that the *PIK3CB* gene is highly expressed in patient cancer specimens and the p110β protein activity plays a critical role during prostate cancer progression as determined in cell culture and nude mouse xenograft models (13). Our data was supported by other groups using *PTEN/PIK3CB* knockout mouse models, as well as cell biology and biochemical experiments (19–22).

In the era of precise medicine, we sought to develop novel targeted therapy for prostate cancer. The very first p110β isoform-specific inhibitor TGX221 was developed in 2005 (23)

based on the structure of a pan-PI3K reversible inhibitor LY294002, which was derived from a natural bio-flavinoid Quercetin (24). In the past few years, we demonstrated that TGX221, either in naked or pro-drug format, inhibited prostate cancer cell proliferation *in vitro* and blocked prostate cancer xenograft tumor growth *in vivo* (25–27). However, TGX221 is not water soluble, representing a huge obstacle for further clinical development. To bypass this roadblock, we recently redesigned and synthesized multiple TGX221 analogs (28) attempted to improve its aqueous solubility while retain its inhibitory effect toward PI3K/p110β. In this study, we tested these TGX221 analogs regarding their aqueous solubility, target engagement and inhibitory effect on PI3K/p110β activity. Our data showed that these TGX221 analogs exerted distinct inhibitory effect on AKT phosphorylation (a typical PI3K downstream event) in multiple prostate-derived cell lines with diverse PI3K/PTEN genetic status, possibly due to their distinct binding specificity to individual PI3K isoforms. One such TGX221 analog, namely BL140, exerted the most superb activities towards PI3K/p110β isoform in terms of target engagement and functional inhibition, comparing to an existing p110β-specific inhibitor GSK2636771 that is being tested in clinical trials. Most significantly, BL140 significantly inhibited cell growth of MDV3100-resistant C4-2B cells by blocking cell cycle entry, indicating that BL140 might be able to eliminate MDV3100 resistant in advanced prostate cancers.

Materials and Methods

Cell lines and reagents

Prostate cancer cell LNCaP, C4-2, 22RV1, DU145 and PC-3 lines were maintained in a humidified atmosphere of 5% CO_2, RPMI1640 media supplemented with 10% fetal bovine serum (FBS) and antibiotics. LNCaP/*shPIK3CB*#3 cell subline was established by stable transfection with a pU6+2-p110βshRNA vector as reported previously (13). C4-2B and its MDV3100-resistant subline cells (C4-2B/MDV-R) were obtained from Dr Allen Gao at UC Davis (29). TGX221 and its analogs were synthesized in house as described previously (28) and the aqueous solubility assay was conducted as reported (30). PI3K inhibitors including BKM120 (catalog #11587), BYL719 (catalog #16986), AZD8186 (catalog #17384), AZD6482 (catalog #15250), GSK2636771 (catalog #17380) and Akt inhibitor VIII (AKT-i8, catalog #14870) were purchased from Cayman Chemicals (Ann Arbor, MI). Antibodies for p110α (clone C73F8), p110β (clone C33D4), p110γ (clone D55D5), VPS34 (clone D4E2), Cyclin D1 (clone 92G2), CDK6 (clone DCS83), $p27^{kip1}$ (catalog #2552), pan-Akt (clone C67E7), phospho-Akt S473 (clone D9E) and T308 (clone 244F9) were obtained from Cell Signaling (Danvers, MA). Antibody for β-Actin (clone AC-15) was purchased from GeneTex Inc (Irvine, CA). Secondary antibodies for mouse and rabbit IgG as well as chemiluminescent reagent kit were purchased from Santa Cruz Biotech (Santa Cruz, CA).

Cellular Thermal Shift Assay

Target engagement of the analogs with PI3K isoform proteins was examined with CETSA assay as described recently (31). Briefly, for cell lysate CETSA, exponentially grown PC-3 cells were harvested and washed with PBS. Cell pellets were suspended in RIPA buffer supplied with protease inhibitor cocktail, followed by a three-cycles of freeze-thaw procedure in liquid nitrogen. The soluble fraction (protein lysate) was separated from the

cell debris by ultra-centrifugation for 20 min at 4°C. Protein aliquots were treated with the compounds or the solvent for 45 min at room temperature, individually heated with gradually increasing temperatures from 37°C to 69°C with 4°C interval for 3 min on a thermal cycler (Bio-Rad, Hercules, CA) and then cooled down at room temperature for 3 min before placed on ice. Insoluble proteins were separated by centrifugation and the soluble proteins were used for Western blot assays.

For whole cell CETSA assay, PC-3 cells were cultured in regular media and treated with the compounds or the solvent for 4 hrs. Cells were washed, harvested in cold PBS. Aliquoted cell pallets were heated at various temperatures (37°C-69°C with 4°C interval) for 3 min and cooled down at room temperature for 2 min before placed on ice. Cell pallets were then suspended in RIPA buffer for three freeze-thaw cycles in liquid nitrogen as described above. Soluble proteins were subjected to Western blot assays.

Signal intensity of Western blot bands were quantified individually using Image J software. Data were normalized by setting the highest and lowest value in each set to 100% and 0%, respectively. The relative signal intensities were plotted against temperature (melting curves) and fitted by applying Boltzmann Sigmoid at least squares using the Graphpad Prism 5.0 software (La Jolla, CA). Thermal shifts were compared using $\Delta T_m 50$ values that were calculated as temperature differences between compound and solvent treatments at a 50% reduction of band density.

Western blot and Kinase-Glo in vitro kinase assays

After treatment, cellular protein lysates were prepared in RIPA buffer (Cell Signaling) supplemented with a complete protease inhibitor cocktail. Equal amount of proteins from each lysate was subjected to SDS-PAGE gels, electrophoresed, and transferred onto PVDF membrane. The membrane was incubated with primary antibody overnight at 4°C after blocking with 10% nonfat dried milk for 1 hr. Membranes were then incubated with horseradish peroxidase-conjugated secondary antibody and immunosignal was developed in a chemiluminescent reagent (Santa Cruz Biotech). Actin blot was used as an internal protein loading control in all blotting membranes.

PI3K activity assays were carried out using the Kinase-Glo Plus luminescent kinase assay kit (Promega catalog #V3773, Madison, WI) coupled with individual active complex of class IA PI3K isoforms including human p110α/p85α (catalog #P27-18-H), human p110β/p85α (catalog #P28-10H) and human p110δ/p85α (P30-102H) obtained from SignalChem (Richmond, Canada). The assays were carried out at 37°C for 2 h in a kinase buffer containing 0.05–0.3 μg enzyme complex, 4 mM DTT, 2 μM ATP and 5 mM PI(4,5)P2:PS substrate (SignalChem catalog #P429-59), as well as the compounds at various concentrations. The luminescent signal was measured using a single tube luminescent device (Berthold Tech, Oak Ridge, TN). Inhibition of PI3K kinase activity by the compounds was calculated with the percentage reduction of luminescent units in compound treatment comparing with that in the solvent control (set as 100%). Inhibitory data of kinase activity were plotted against the compound concentrations, IC_{50} values were calculated and curve were fitted using sigmoidal dose-response with variable slope (GraphPad Prism 5.0 software).

Flow cytometry and cell growth inhibition assay

For cell cycle analysis, cells were serum-starved for 24 hr and were returned to serum-containing media (10% FBS) with the solvent or compounds for various periods as indicated in the figures. After trypsinization, cells were fixed and stained with propidium iodide (PI). PI-labeled cells were counted using a fluorescence activated cell sorter BD LSR II (BD Biosciences, San Jose, CA) and cell cycle distribution was calculated with the Flow Jo software.

For cell growth inhibition, cells were seeded at a density of 8,000 cells per well in 96-well culture plates and allowed to grow for 24 hrs followed by treatment with increasing concentrations of the testing compounds for 3 days. WST-8 mixture from the WST-8 Cell Proliferation Assay Kit (Cayman chemical) was added to each well and incubated for 2 hrs at 37°C. Optical density (OD) values were measured at 450 nm on a Multiskan Ascent plate reader (Thermo Labsystems, Beverly, MA). The curve fit was conducted by applying compound concentration (log value) vs. normalized inhibitory response (percentage value) with variable slope and EC_{50} values were calculated using Graphpad Prism 5.0 software.

Statistical analysis

Data were present as the mean and SEM from at least three repeated experiments for all of the quantitative assays. Western blot data were shown from a representative experiment. Statistical analysis was conducted using one-way ANOVA analysis with SPSS software (Chicago, IL). A student t-test was performed to compare two groups and a p value of 0.05 was considered to indicate a significant difference.

Results

TGX221 analogs exerts a high solubility in aqueous solution

TGX221 has been used as an anti-thrombotic and anti-tumor agent *in vitro* and *in vivo* [25, 47, 62–64]. However, the clinical development of TGX221 as an anti-cancer drug was hampered due to its poor water solubility (< 1.0 mg/ml). To overcome this obstacle, we redesigned and synthesized multiple TGX221 analogs (28), as illustrated in Fig 1. As expected, replacing either one of two major functional groups circled in red or blue dashed lines in TGX221 by more hydrophilic groups, their aqueous solubility was dramatically improved compared to TGX221 (about 40-fold increase, Tab 1). It was also over 70-fold higher compared to the compound SAR260301 (0.928 mM) (32,33) that was recently tested in clinical trial (NCT01673737). These promising data encouraged us to conduct a detailed characterization of these analogs in prostate cancer cells.

TGX221 analogs exert a high specificity of target engagement

We first utilized the cellular thermal shift assay (CETSA) (34) to determine the engagement of TGX221 analogs with the target protein p110β, as well as other PI3K isoforms if any. To eliminate potential interplays among cellular proteins in living cells, we used PC-3 cellular protein lysates for these CETSA assays according to the published protocol (31). Our data revealed that TGX221 and its four analogs dramatically altered p110β thermos-melting curve comparing to the solvent control (Fig 2B). In contrast, none of them largely shifted the

thermo-melting curves of other class I PI3K proteins p110α (Fig 2A) and p110γ (Fig 2C), as well as their major downstream target Akt protein (Fig 2E), although the compound BL147 moderately changed the melting curve of class III PI3K VPS34 protein (Fig 2D).

Then, we verified the p110β engagement properties of the TGX221 analogs in living cells. Exponentially grown PC-3 cells were treated with these compounds for 2 h and harvested for the CETSA assays. Similar as the *in vitro* CETSA assay data, these analogs strongly altered the thermo-melting curve of p110β protein (Fig 2F) but not Akt protein (Fig 2G). The ΔT_m50 values for all analogs were summarized in Tab 2. These data suggest that these TGX221 analogs are specifically engaged with PI3K class IA p110β protein except BL147 also for VPS34.

TGX221 analog BL140 exerts a unified PI3K inhibitory effect

We continued on determining the functional effect of these TGX221 analogs on Akt serine-473 (S473) phosphorylation, a major PI3K downstream activity readout. Four prostate cancer cell lines were tested including two androgen receptor (AR)-negative (PC-3 and DU145) and two AR-positive (22RV1 and C4-2) cell lines. Cells were serum-starved overnight to reduce AKT phosphorylation events. After a 30-min pretreatment with the solvent or TGX221 analogs, cells were stimulated with 10% FBS. AKT S473 phosphorylation (pS473) was evaluated by Western blotting. As shown in Fig 3A–3D, all cell lines responded to FBS stimulation nicely with increased AKT S473 phosphorylation but differently to the analog pre-treatment. Among these TGX221 analogs, BL140 exerted a unified inhibitory effect on Akt pS473 in all cell lines tested (Fig 3E). These data strongly indicate that the BL140 analog is the best candidate of PI3K/p110β-specific inhibitor among these TGX221 analogs.

BL140 possesses a highly p110β specificity

We next examined the BL140 specificity towards p110β with two different approaches. First, BL140's specificity and efficiency was tested in an *in vitro* Kinase-Glo luminescent kinase assay coupled with purified recombinant class IA PI3K/p110x-p85α active protein mixture. Two previously reported PI3K inhibitors, BYL719 for p110α (35) and GSK2636771 for p110β (36), were used as the isoform specificity control. As expected, BYL719 showed a very specific effect on p110α activity (Fig 4A) and GSK2636771 on p110β (Fig 4B). However, GSK2636771 also exerted inhibitory effect on p110δ (Fig 4C & Tab 3). Interestingly, BL140 showed a very high specificity on p110β, similar as its predecessor TGX221 but a sharply weak inhibitory effect on p110α (150-fold weaker) or p110δ (745-fold weaker). The IC_{50} values for all these compounds were summarized in Tab 3.

The second approach to test BL140 specificity on p110β was conducted on LNCaP and its subline LNCaP/shPIK3CB#3, which was established in our previous work by stably transfecting with a *PIK3CB* gene small-hairpin interfering RNA construct (13). We reasoned that in a p110β-less cell, a given p110β-specific inhibitor will show a very limited inhibitory effect on Akt S473 phosphorylation since the target is missing. LNCaP and LNCaP/shPIK3CB#3 cells were treated with multiple PI3K inhibitors at 5 μM for 4 h before

harvested for Akt pS473 evaluation. As shown in Fig 4D, in LNCaP cells, the broad PI3K inhibitor BKM120 and AKT-specific inhibitor AKT-i8, together with AZD8186 and AZD6482, completely abolished Akt pS473 event. In contrast, isoform-selective inhibitors BYL719, TGX221, BL140 and GSK2636771 all showed a partial inhibitory effect on Akt pS473 level. In LNCaP/shPIK3CB#3 cells (Fig 4E), BKM120 and AKT-i8 retained their full capacity on Akt pS473 inhibition but AZD8186 and AZD6482 only partially inhibited Akt pS473 levels. Most significantly, TGX221, BL140 and GSK2636771 all lost their inhibitory effect on Akt pS473 levels, a strong indication of their p11β specificity. The relative band densities were summarized in Fig 4F. These data clearly demonstrated that BL140 is a very strong and specific p110β inhibitor *in vitro* and *in vivo*, similar as its predecessor TGX221 but better than GSK2636771. The target specificity for AZD8186 and AZD6482 needs further characterization in detail.

BL140 inhibits cell growth of castration-resistant prostate cancer cells

Lastly, we examined the anti-cancer effect of BL140 in comparison to GSK2636771 in castration-resistant prostate cancer cells. 22RV1 (PTEN positive with AR variants), PC-3 (PTEN/AR negative) and C4-2B (PTEN null with AR mutant) cell lines were treated with the compounds and cell growth was evaluated with the WST-8 assay. A MDV3100 (Enzalutamide)-resistant C4-2B cell subline (29) was also included in the testing. As shown in Fig 5A–5D, all three compounds significantly suppressed cell growth in a dose-dependent manner and the responsiveness order as evaluated by compound EC_{50} values was listed as follow: PC-3 > 22RV1 > C4-2B > C4-2B/MDV-R (Tab 4). For all cell lines tested, BL140 showed a similar efficiency as TGX221 but a much better performance than GSK2636771.

We also analyzed cell cycle phase distribution in C4-2B and its MDV3100-resistant subline to understand the mechanism of cell growth suppression. Cells were synchronized by serum starvation overnight. After a 30-min pretreatment with the compounds, cells were stimulated with 10% FBS and harvested at 16 h later for flow cytometry-based cell cycle analysis. As shown in Fig 5E–5F, both MDV3100-sensitive (C4-2B) and -resistant (C4-2B/MDV-R) cells showed a similar cell cycle distribution in the solvent control, indicating MDV3100 resistance in C4-2B/MDV-R cells. However, treatment with TGX221, BL140 or GSK2636771 significantly increased G_0/G_1 population accompanied with a large reduction of S-phase cells not only in C4-2B cells but also in C4-2B/MDV-R cells, although the extent of G_1/G_0 phase arrest in MDV-R cells was less than that in the parental C4-2B cells (Fig 5G–5H). These data suggest that G_0/G_1 arrest is responsible for these p110β-specific inhibitors-induced cell growth suppression.

We then compared the Akt pS473 status between these pair of C4-2B cells in response to BL140 and GSK2636771 treatment. C4-2B and its MDV-R subline cells were serum-starved overnight and then pre-treated with the compounds followed by addition of 10% FBS. As shown in Fig 6A, FBS-stimulated Akt pS473 levels in C4-2B cells were abolished by BL140 or GSK2636771 treatment but were enhanced by MDV3100 treatment, which was supported by previous reports that Akt activity was increased by AR antagonist (14,16). In MDV-R cells, BL140 abolished FBS-stimulated Akt pS473, however, GSK2636771 only partially

suppressed FBS-stimulated Akt pS473 phosphorylation (Fig 6B). These data indicate that BL140 is superior on PI3K/AKT inhibition than GSK2636771 in MDV3100-resistant cells.

To understand the mechanism for G_1/G_0 phase arrest, we analyzed the protein levels of three major factors for G_1 phase progression, cyclin D1, CDK6 and $p27^{kip1}$. In both MDV3100-sensitive and -resistant C4-2B cell lines, cyclin D1 protein levels in control treatment were gradually increased with time after FBS addition, a sign of G_1 phase progression. Interestingly, this increase was largely suppressed by BL140 or GSK2636771 treatment, indicating a potential association of cyclin D1 reduction in G_1 phase arrest induced by BL140 and GSK2636771. Meanwhile, $p27^{kip1}$ protein levels were largely elevated in BL140- or GSK2636771-treated C4-2B cells but not in C4-2B/MDV-R cells. There was no obvious alteration of CDK6 protein levels between the control and compound treatments in MDV3100-sensitive or MDV3100-resistant C4-2B cells. These data suggest that p110β inhibition with BL140 or GSK2636771 eliminates MDV3100 resistance in castration-resistant prostate cancer cells by blocking cell cycle progression through cyclin D1 protein reduction. Further *in vivo* testing in animal models are underway by our group.

Discussion

In this study, we characterized four novel TGX221 analogs (BL139, BL140, BL141 and BL147) for their aqueous solubility, target engagement and functional efficiency in prostate cancer cells. Our data demonstrated that BL140 possesses the best and favorable properties in target specificity towards p110β and better functional efficiency compared to existing p110β specific inhibitor GSK2636771, although other analogs also have a drastic improvement in aqueous solubility compared to the parent compound TGX221. The IC_{50} of *in vitro* p110β kinase activity for BL140 is 5.744 nM, which is almost 4-fold lower than GSK2636771 (20.49 nM). Most significantly, the EC_{50} for BL140 in suppressing prostate cancer cell growth is much lower than that of GSK2636771 in all prostate cancer cell lines tested. Interestingly, in MDV3100-resistant C4-2B cells that are closely related to current clinical obstacle, BL140 treatment significantly inhibited cell growth, a sign of eliminating MDV3100 resistance. Mechanistic studies revealed that BL140 treatment caused a significant G_1/G_0 cell cycle arrest in parallel with a reduction of S-phase population in both MDV3100-sensitive and -resistant C4-2B cells, which is supported by previous report that p110β is involved in regulating G_1 phase progression (37). Further analysis indicated that BL140-induced G_1/G_0 arrest was associated with a significant decrease of cyclin D1 protein, the major G_1 driving force. However, BL140-induced accumulation of $p27^{kip1}$ protein, a negative G_1 phase regulator, was only observed in MDV3100-sensitive but not in MDV3100-resistant C4-2B cells, suggesting an interplay between p110β inhibitors and MDV3100 on $p27^{kip1}$ protein levels in prostate cancer cells.

Currently, targeting the PI3K pathway with isoform-specific inhibitors has been the major development in the field of cancer therapeutics (38). As the very first PI3K/p110β-specific inhibitor, TGX221 has been used as an anti-thrombotic and anti-tumor agent *in vitro* and *in vivo* (39–42). Works from our group with TGX221-loaded prostate-cancer cell-homing nano-micelles documented the growth blockage of mouse orthotopic xenograft tumors derived from advanced prostate cancer cells (25,26), confirming the feasibility of p110β-

targeted therapy for prostate cancer intervention. Although multiple p110β-specific inhibitors were reported (43,44), only GSK2636771 proceeded to phase-2 clinical trial (NCT01458067) for PTEN-negative solid tumors and another phase-1 trial is ongoing to test the combinational treatment of GSK2636771 plus MDV3100 in metastatic CRPC patients (NCT02215096). Another PI3K/p110β-specific inhibitor SAR260301 was failed in phase-1 trial (NCT01673737) due to severe side effect (45). In this study, we demonstrated that the novel TGX221 analog BL140 possesses multiple favorable properties for clinical development as an anti-cancer therapy for PTEN-negative or p110β-prone cancers. Our unpublished preliminary data also indicated that BL140 was very stable even in acidic solution that mimics human gastric secretion, suggesting a potential and convenient oral route for drug delivery.

MDV3100, also termed as Enzalutamide, is the latest AR antagonist in clinic, unfortunately, drug resistance has already become a critical issue in CRPC patients. Although the mechanisms underlying MDV3100 resistance remains incomplete known, the existence of AR variants that lack ligand binding domain has been pointed as the major cause (46–48). In this study, we demonstrated that BL140 treatment led to G_1 phase arrest and cyclin D1 protein reduction not only in MDV3100-sensitive but also in MDV3100-resistant aggressive CRPC C4-2B cells. PTEN/PI3K-Akt pathway has been shown as the major cellular pathway in regulating cell cycle entry and cyclin D1 protein levels possibly through GSK-3 dependent proteolysis (49,50). Disturbing this pathway, for example, PI3K inhibition, would result in cyclin D1 depletion and cell cycle arrest (51). In addition, AR antagonist treatment was shown to enhance PI3K/AKT activity (14,16), therefore, blocking PI3K/p110β-Akt activation with BL140 could be used as a potential MDV3100 sensitizing agent for CRPCs as recently reported with Akt-specific inhibitor AZD5363 (52,53).

In conclusion, we characterized a group of novel TGX21 analogs with greatly improved aqueous solubility compared to the parent compound. One of the analogs BL140 possesses a consistent inhibitory effect on PI3K/AKT activity in multiple prostate cancer cell lines with diverse genetic background. BL140 is superior than GSK2636771 either in kinase inhibition or in cell growth suppression. BL140 suppressed cell growth and blocks cell cycle entry not only in MDV3100-sensitive but also in MDV3100-ressistant C4-2B cells by reducing cyclin D1 protein levels. These data strongly indicate that BL140 is a promising candidate for further clinical development as a combined therapy with MDV3100 for CRPC patients.

Acknowledgments

We thank Mr Richard Hastings for his excellent technical assistance in flow cytometry analysis of cell cycle distribution and the Flow Cytometry Core Laboratory at KUMC. This study was mainly supported by KU Cancer Center Drug Discovery pilot grant (D3ET-FY2015) and a KU-NIH/NCRR COBRE grant (1P20RR15563) to Dr Benyi Li. This work was also partially supported by a grant from Kansas Board of Regents (FY2016 to Dr Benyi Li as a Co-Investigator) and a grant from the National Natural Science Foundation of Henan Province (grant #162300410044) to Dr Shaofeng Duan. The Flow Cytometry Core Laboratory at KUMC is partially sponsored by grants from NIH/NIGMS COBRE (P30GM103326) and NIH/NCRR (P20RR016443).

Abbreviation

ACPP prostate-specific acid phosphatase

AR	androgen receptor
CETSA	cellular thermal shift assay
CRPC	castration-resistant prostate cancer
FBS	fetal bovine serum
MDV-R	MDV3100 resistant
OD	optical density
PI	propidium iodide
PI3K	Phosphatidylinositol 3-kinase
PTEN	phosphatase and tensin homologue deleted on chromosome 10
RIPA	radio-immunoprecipitation assay

References

1. Scher HI, Sawyers CL. Biology of progressive, castration-resistant prostate cancer: directed therapies targeting the androgen-receptor signaling axis. J Clin Oncol. 2005; 23(32):8253–8261. [PubMed: 16278481]
2. Scher HI, Fizazi K, Saad F, Taplin ME, Sternberg CN, Miller K, de Wit R, Mulders P, Chi KN, Shore ND, Armstrong AJ, Flaig TW, Flechon A, Mainwaring P, Fleming M, Hainsworth JD, Hirmand M, Selby B, Seely L, de Bono JS. Investigators A. Increased survival with enzalutamide in prostate cancer after chemotherapy. N Engl J Med. 2012; 367(13):1187–1197. [PubMed: 22894553]
3. de Bono JS, Logothetis CJ, Molina A, Fizazi K, North S, Chu L, Chi KN, Jones RJ, Goodman OB Jr, Saad F, Staffurth JN, Mainwaring P, Harland S, Flaig TW, Hutson TE, Cheng T, Patterson H, Hainsworth JD, Ryan CJ, Sternberg CN, Ellard SL, Flechon A, Saleh M, Scholz M, Efstathiou E, Zivi A, Bianchini D, Loriot Y, Chieffo N, Kheoh T, Haqq CM, Scher HI. Investigators C-A. Abiraterone and increased survival in metastatic prostate cancer. N Engl J Med. 2011; 364(21): 1995–2005. [PubMed: 21612468]
4. Kantoff PW, Higano CS, Shore ND, Berger ER, Small EJ, Penson DF, Redfern CH, Ferrari AC, Dreicer R, Sims RB, Xu Y, Frohlich MW, Schellhammer PF. Investigators IS. Sipuleucel-T immunotherapy for castration-resistant prostate cancer. N Engl J Med. 2010; 363(5):411–422. [PubMed: 20818862]
5. Thorpe LM, Yuzugullu H, Zhao JJ. PI3K in cancer: divergent roles of isoforms, modes of activation and therapeutic targeting. Nat Rev Cancer. 2015; 15(1):7–24. [PubMed: 25533673]
6. Ilic N, Roberts TM. Comparing the roles of the p110alpha and p110beta isoforms of PI3K in signaling and cancer. Curr Top Microbiol Immunol. 2010; 347:55–77. [PubMed: 20517719]
7. Burke JE, Williams RL. Synergy in activating class I PI3Ks. Trends Biochem Sci. 2015; 40(2):88–100. [PubMed: 25573003]
8. Sopasakis VR, Liu P, Suzuki R, Kondo T, Winnay J, Tran TT, Asano T, Smyth G, Sajan MP, Farese RV, Kahn CR, Zhao JJ. Specific roles of the p110alpha isoform of phosphatidylinsositol 3-kinase in hepatic insulin signaling and metabolic regulation. Cell Metab. 2010; 11(3):220–230. [PubMed: 20197055]
9. Li J, Yen C, Liaw D, Podsypanina K, Bose S, Wang SI, Puc J, Miliaresis C, Rodgers L, McCombie R, Bigner SH, Giovanella BC, Ittmann M, Tycko B, Hibshoosh H, Wigler MH, Parsons R. PTEN, a putative protein tyrosine phosphatase gene mutated in human brain, breast, and prostate cancer. Science. 1997; 275(5308):1943–1947. [PubMed: 9072974]

10. Berenjeno IM, Guillermet-Guibert J, Pearce W, Gray A, Fleming S, Vanhaesebroeck B. Both p110alpha and p110beta isoforms of PI3K can modulate the impact of loss-of-function of the PTEN tumour suppressor. Biochem J. 2012; 442(1):151–159. [PubMed: 22150431]
11. Fraser M, Berlin A, Bristow RG, van der Kwast T. Genomic, pathological, and clinical heterogeneity as drivers of personalized medicine in prostate cancer. Urol Oncol. 2015; 33(2):85–94. [PubMed: 24768356]
12. Robinson D, Van Allen EM, Wu YM, Schultz N, Lonigro RJ, Mosquera JM, Montgomery B, Taplin ME, Pritchard CC, Attard G, Beltran H, Abida W, Bradley RK, Vinson J, Cao X, Vats P, Kunju LP, Hussain M, Feng FY, Tomlins SA, Cooney KA, Smith DC, Brennan C, Siddiqui J, Mehra R, Chen Y, Rathkopf DE, Morris MJ, Solomon SB, Durack JC, Reuter VE, Gopalan A, Gao J, Loda M, Lis RT, Bowden M, Balk SP, Gaviola G, Sougnez C, Gupta M, Yu EY, Mostaghel EA, Cheng HH, Mulcahy H, True LD, Plymate SR, Dvinge H, Ferraldeschi R, Flohr P, Miranda S, Zafeiriou Z, Tunariu N, Mateo J, Perez-Lopez R, Demichelis F, Robinson BD, Schiffman M, Nanus DM, Tagawa ST, Sigaras A, Eng KW, Elemento O, Sboner A, Heath EI, Scher HI, Pienta KJ, Kantoff P, de Bono JS, Rubin MA, Nelson PS, Garraway LA, Sawyers CL, Chinnaiyan AM. Integrative clinical genomics of advanced prostate cancer. Cell. 2015; 161(5):1215–1228. [PubMed: 26000489]
13. Zhu Q, Youn H, Tang J, Tawfik O, Dennis K, Terranova PF, Du J, Raynal P, Thrasher JB, Li B. Phosphoinositide 3-OH kinase p85alpha and p110beta are essential for androgen receptor transactivation and tumor progression in prostate cancers. Oncogene. 2008; 27(33):4569–4579. [PubMed: 18372911]
14. Carver BS, Chapinski C, Wongvipat J, Hieronymus H, Chen Y, Chandarlapaty S, Arora VK, Le C, Koutcher J, Scher H, Scardino PT, Rosen N, Sawyers CL. Reciprocal feedback regulation of PI3K and androgen receptor signaling in PTEN-deficient prostate cancer. Cancer Cell. 2011; 19(5):575–586. [PubMed: 21575859]
15. Schwartz S, Wongvipat J, Trigwell CB, Hancox U, Carver BS, Rodrik-Outmezguine V, Will M, Yellen P, de Stanchina E, Baselga J, Scher HI, Barry ST, Sawyers CL, Chandarlapaty S, Rosen N. Feedback suppression of PI3Kalpha signaling in PTEN-mutated tumors is relieved by selective inhibition of PI3Kbeta. Cancer Cell. 2015; 27(1):109–122. [PubMed: 25544636]
16. Qi W, Morales C, Cooke LS, Johnson B, Somer B, Mahadevan D. Reciprocal feedback inhibition of the androgen receptor and PI3K as a novel therapy for castrate-sensitive and -resistant prostate cancer. Oncotarget. 2015; 6(39):41976–41987. [PubMed: 26506516]
17. Lee SH, Johnson D, Luong R, Sun Z. Crosstalking between androgen and PI3K/AKT signaling pathways in prostate cancer cells. J Biol Chem. 2015; 290(5):2759–2768. [PubMed: 25527506]
18. Munkley J, Livermore KE, McClurg UL, Kalna G, Knight B, McCullagh P, McGrath J, Crundwell M, Leung HY, Robson CN, Harries LW, Rajan P, Elliott DJ. The PI3K regulatory subunit gene PIK3R1 is under direct control of androgens and repressed in prostate cancer cells. Oncoscience. 2015; 2(9):755–764. [PubMed: 26501081]
19. Jia S, Liu Z, Zhang S, Liu P, Zhang L, Lee SH, Zhang J, Signoretti S, Loda M, Roberts TM, Zhao JJ. Essential roles of PI(3)K-p110beta in cell growth, metabolism and tumorigenesis. Nature. 2008; 454(7205):776–779. [PubMed: 18594509]
20. Wee S, Wiederschain D, Maira SM, Loo A, Miller C, deBeaumont R, Stegmeier F, Yao YM, Lengauer C. PTEN-deficient cancers depend on PIK3CB. Proc Natl Acad Sci U S A. 2008; 105(35):13057–13062. [PubMed: 18755892]
21. Jiang X, Chen S, Asara JM, Balk SP. Phosphoinositide 3-kinase pathway activation in phosphate and tensin homolog (PTEN)-deficient prostate cancer cells is independent of receptor tyrosine kinases and mediated by the p110beta and p110delta catalytic subunits. J Biol Chem. 2010; 285(20):14980–14989. [PubMed: 20231295]
22. Lee SH, Poulogiannis G, Pyne S, Jia S, Zou L, Signoretti S, Loda M, Cantley LC, Roberts TM. A constitutively activated form of the p110beta isoform of PI3-kinase induces prostatic intraepithelial neoplasia in mice. Proc Natl Acad Sci U S A. 2010; 107(24):11002–11007. [PubMed: 20534477]
23. Jackson SP, Schoenwaelder SM, Goncalves I, Nesbitt WS, Yap CL, Wright CE, Kenche V, Anderson KE, Dopheide SM, Yuan Y, Sturgeon SA, Prabaharan H, Thompson PE, Smith GD, Shepherd PR, Daniele N, Kulkarni S, Abbott B, Saylik D, Jones C, Lu L, Giuliano S, Hughan SC,

Angus JA, Robertson AD, Salem HH. PI 3-kinase p110beta: a new target for antithrombotic therapy. Nat Med. 2005; 11(5):507–514. [PubMed: 15834429]

24. Vlahos CJ, Matter WF, Hui KY, Brown RF. A specific inhibitor of phosphatidylinositol 3-kinase, 2-(4-morpholinyl)-8-phenyl-4H-1-benzopyran-4-one (LY294002). The Journal of biological chemistry. 1994; 269(7):5241–5248. [PubMed: 8106507]
25. Chen R, Zhao Y, Huang Y, Yang Q, Zeng X, Jiang W, Liu J, Thrasher JB, Forrest ML, Li B. Nanomicellar TGX221 blocks xenograft tumor growth of prostate cancer in nude mice. Prostate. 2015; 75(6):593–602. [PubMed: 25620467]
26. Zhao Y, Duan S, Zeng X, Liu C, Davies NM, Li B, Forrest ML. Prodrug strategy for PSMA-targeted delivery of TGX-221 to prostate cancer cells. Mol Pharm. 2012; 9(6):1705–1716. [PubMed: 22494444]
27. Tai W, Shukla RS, Qin B, Li B, Cheng K. Development of a peptide-drug conjugate for prostate cancer therapy. Mol Pharm. 2011; 8(3):901–912. [PubMed: 21510670]
28. Liu CJ, Li BY, Mitscher L. Synthesis of New TGX-221 Analogs. Z Naturforsch B. 2014; 69(7): 817–822.
29. Liu C, Lou W, Armstrong C, Zhu Y, Evans CP, Gao AC. Niclosamide suppresses cell migration and invasion in enzalutamide resistant prostate cancer cells via Stat3-AR axis inhibition. Prostate. 2015; 75(13):1341–1353. [PubMed: 25970160]
30. Kerns EH, Di L, Carter GT. In vitro solubility assays in drug discovery. Curr Drug Metab. 2008; 9(9):879–885. [PubMed: 18991584]
31. Jafari R, Almqvist H, Axelsson H, Ignatushchenko M, Lundback T, Nordlund P, Martinez Molina D. The cellular thermal shift assay for evaluating drug target interactions in cells. Nat Protoc. 2014; 9(9):2100–2122. [PubMed: 25101824]
32. Bonnevaux H, Lemaitre O, Vincent L, Levit MN, Windenberger F, Halley F, Delorme C, Lengauer C, Garcia-Echeverria C, Virone-Oddos A. Concomitant Inhibition of PI3Kb and BRAF or MEK in PTEN-Deficient/BRAF-Mutant Melanoma Treatment: Preclinical Assessment of SAR260301 Oral PI3K beta-Selective Inhibitor. Molecular Cancer Therapeutics. 2016; 15(7):1460–1471. [PubMed: 27196754]
33. Certal V, Carry JC, Halley F, Virone-Oddos A, Thompson F, Filoche-Romme B, El-Ahmad Y, Karlsson A, Charrier V, Delorme C, Rak A, Abecassis PY, Amara C, Vincent L, Bonnevaux H, Nicolas JP, Mathieu M, Bertrand T, Marquette JP, Michot N, Benard T, Perrin MA, Lemaitre O, Guerif S, Perron S, Monget S, Gruss-Leleu F, Doerflinger G, Guizani H, Brollo M, Delbarre L, Benin L, Richepin P, Loyau V, Garcia-Echeverria C, Lengauer C, Schio L. Discovery and Optimization of Pyrimidone Indoline Amide P13K beta Inhibitors for the Treatment of Phosphatase and Tensin Homologue (PTEN)-Deficient Cancers. J Med Chem. 2014; 57(3):903–920. [PubMed: 24387221]
34. Martinez Molina D, Jafari R, Ignatushchenko M, Seki T, Larsson EA, Dan C, Sreekumar L, Cao Y, Nordlund P. Monitoring drug target engagement in cells and tissues using the cellular thermal shift assay. Science. 2013; 341(6141):84–87. [PubMed: 23828940]
35. Furet P, Guagnano V, Fairhurst RA, Imbach-Weese P, Bruce I, Knapp M, Fritsch C, Blasco F, Blanz J, Aichholz R, Hamon J, Fabbro D, Caravatti G. Discovery of NVP-BYL719 a potent and selective phosphatidylinositol-3 kinase alpha inhibitor selected for clinical evaluation. Bioorg Med Chem Lett. 2013; 23(13):3741–3748. [PubMed: 23726034]
36. Weigelt B, Warne PH, Lambros MB, Reis-Filho JS, Downward J. PI3K pathway dependencies in endometrioid endometrial cancer cell lines. Clin Cancer Res. 2013; 19(13):3533–3544. [PubMed: 23674493]
37. Marques M, Kumar A, Cortes I, Gonzalez-Garcia A, Hernandez C, Moreno-Ortiz MC, Carrera AC. Phosphoinositide 3-kinases p110alpha and p110beta regulate cell cycle entry, exhibiting distinct activation kinetics in G1 phase. Mol Cell Biol. 2008; 28(8):2803–2814. [PubMed: 18285463]
38. Mayer IA, Arteaga CL. The PI3K/AKT Pathway as a Target for Cancer Treatment. Annu Rev Med. 2016; 67:11–28. [PubMed: 26473415]
39. Sturgeon SA, Jones C, Angus JA, Wright CE. Advantages of a selective beta-isoform phosphoinositide 3-kinase antagonist, an anti-thrombotic agent devoid of other cardiovascular

actions in the rat. European journal of pharmacology. 2008; 587(1–3):209–215. [PubMed: 18455722]

40. Edgar KA, Wallin JJ, Berry M, Lee LB, Prior WW, Sampath D, Friedman LS, Belvin M. Isoform-specific phosphoinositide 3-kinase inhibitors exert distinct effects in solid tumors. Cancer research. 2010; 70(3):1164–1172. [PubMed: 20103642]
41. Bird JE, Smith PL, Bostwick JS, Shipkova P, Schumacher WA. Bleeding response induced by anti-thrombotic doses of a phosphoinositide 3-kinase (PI3K)-beta inhibitor in mice. Thromb Res. 2011; 127(6):560–564. [PubMed: 21396684]
42. Feng C, Sun Y, Ding G, Wu Z, Jiang H, Wang L, Ding Q, Wen H. PI3Kbeta inhibitor TGX221 selectively inhibits renal cell carcinoma cells with both VHL and SETD2 mutations and links multiple pathways. Sci Rep. 2015; 5:9465. [PubMed: 25853938]
43. Liu Y, Wan WZ, Li Y, Zhou GL, Liu XG. Recent development of ATP-competitive small molecule phosphatidylinostitol-3-kinase inhibitors as anticancer agents. Oncotarget. 2017; 8(4):7181–7200. [PubMed: 27769061]
44. Li B, Sun A, Jiang W, Thrasher JB, Terranova P. PI-3 kinase p110beta: a therapeutic target in advanced prostate cancers. Am J Clin Exp Urol. 2014; 2(3):188–198. [PubMed: 25374921]
45. Bedard PL, Davies MA, Kopetz S, Flaherty KT, Shapiro G, Luke JJ, Spreafico A, Wu B, Gomez C, Cartot-Cotton S, Mazuir F, Micallef S, Demers B, Juric D. First-in-human phase I trial of the PI3Kb-selective inhibitor SAR260301 in patients with advanced solid tumors (NCT01673737). Journal of Clinical Oncology. 2015; 33(15)
46. Antonarakis ES, Lu C, Wang H, Luber B, Nakazawa M, Roeser JC, Chen Y, Mohammad TA, Chen Y, Fedor HL, Lotan TL, Zheng Q, De Marzo AM, Isaacs JT, Isaacs WB, Nadal R, Paller CJ, Denmeade SR, Carducci MA, Eisenberger MA, Luo J. AR-V7 and resistance to enzalutamide and abiraterone in prostate cancer. N Engl J Med. 2014; 371(11):1028–1038. [PubMed: 25184630]
47. Cao B, Qi Y, Zhang G, Xu D, Zhan Y, Alvarez X, Guo Z, Fu X, Plymate SR, Sartor O, Zhang H, Dong Y. Androgen receptor splice variants activating the full-length receptor in mediating resistance to androgen-directed therapy. Oncotarget. 2014; 5(6):1646–1656. [PubMed: 24722067]
48. Nadiminty N, Tummala R, Liu C, Yang J, Lou W, Evans CP, Gao AC. NF-kappaB2/p52 induces resistance to enzalutamide in prostate cancer: role of androgen receptor and its variants. Mol Cancer Ther. 2013; 12(8):1629–1637. [PubMed: 23699654]
49. Radu A, Neubauer V, Akagi T, Hanafusa H, Georgescu MM. PTEN induces cell cycle arrest by decreasing the level and nuclear localization of cyclin D1. Mol Cell Biol. 2003; 23(17):6139–6149. [PubMed: 12917336]
50. Diehl JA, Cheng M, Roussel MF, Sherr CJ. Glycogen synthase kinase-3beta regulates cyclin D1 proteolysis and subcellular localization. Genes Dev. 1998; 12(22):3499–3511. [PubMed: 9832503]
51. Shukla S, Gupta S. Apigenin-induced cell cycle arrest is mediated by modulation of MAPK, PI3K-Akt, and loss of cyclin D1 associated retinoblastoma dephosphorylation in human prostate cancer cells. Cell Cycle. 2007; 6(9):1102–1114. [PubMed: 17457054]
52. Toren P, Kim S, Cordonnier T, Crafter C, Davies BR, Fazli L, Gleave ME, Zoubeidi A. Combination AZD5363 with Enzalutamide Significantly Delays Enzalutamide-resistant Prostate Cancer in Preclinical Models. Eur Urol. 2015; 67(6):986–990. [PubMed: 25151012]
53. Thomas C, Lamoureux F, Crafter C, Davies BR, Beraldi E, Fazli L, Kim S, Thaper D, Gleave ME, Zoubeidi A. Synergistic targeting of PI3K/AKT pathway and androgen receptor axis significantly delays castration-resistant prostate cancer progression in vivo. Mol Cancer Ther. 2013; 12(11): 2342–2355. [PubMed: 23966621]

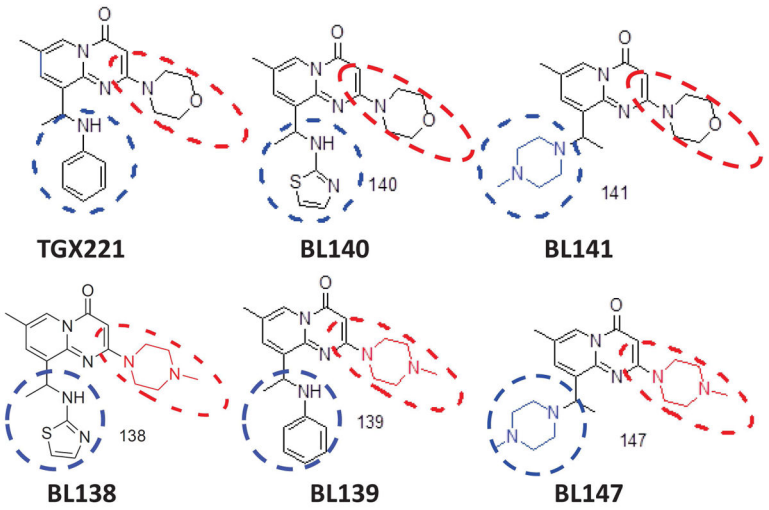

Fig 1.

Chemical structure of TGX221 and its analogs. Two major functional groups were circled in red or blue dashed lines.

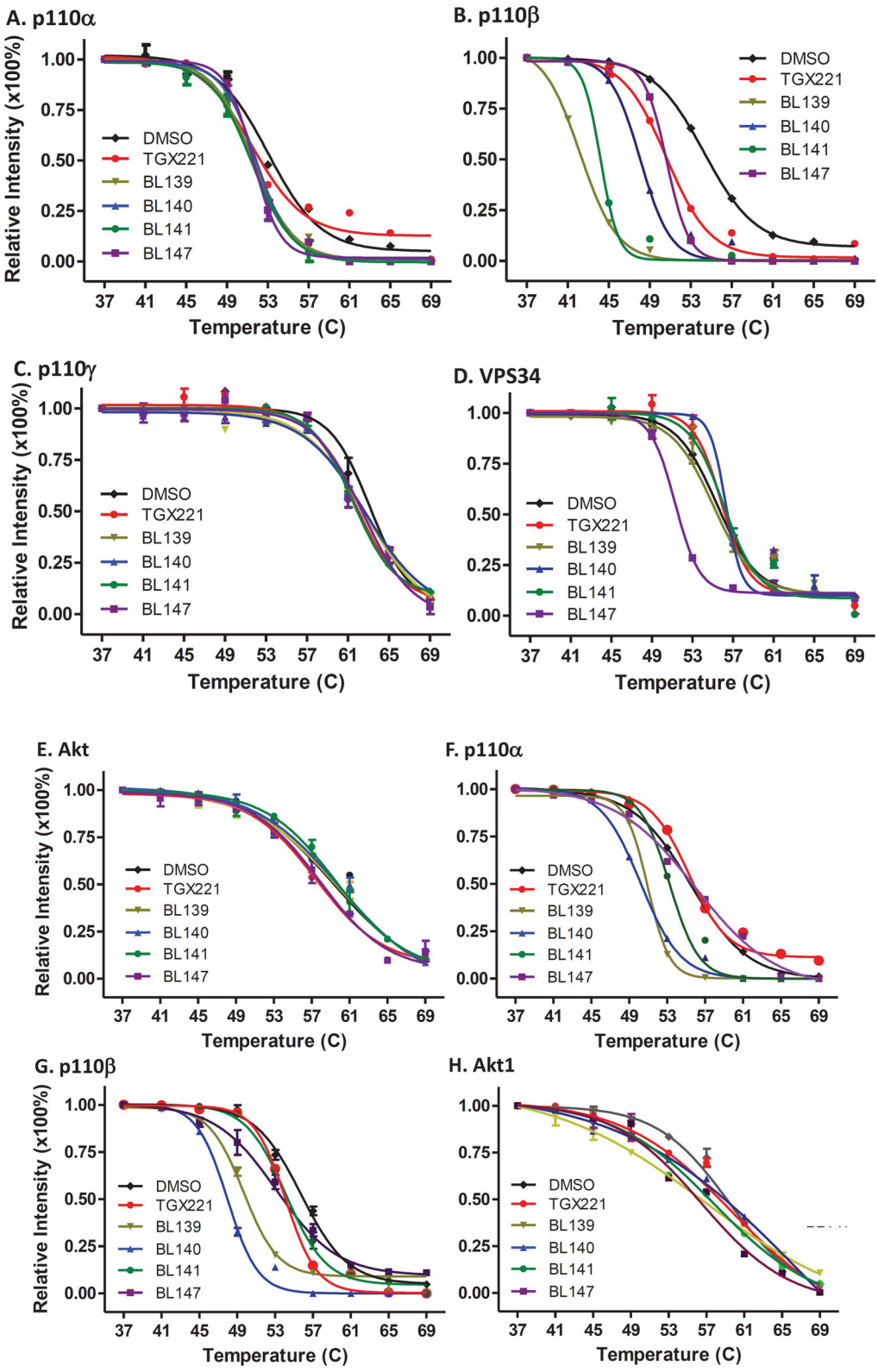

Fig 2.

TGX221 and its analogs are specifically engaged with PI3K p110β protein. Cellular protein lysates from exponentially grown PC-3 cells were mixed with the solvent DMSO or the compounds at 5 μM for 30 min followed by CETSA assay as described (31). Panel **A–E** are from cell lysate CETSA and panel **F–H** are for whole cell CETSA. The signal intensity of bands was quantified using Image J. Data were then normalized by setting the highest and lowest value in each set to 100% and 0%, respectively. The relative signal intensities (protein melting curves) were plotted against temperatures using GraphPad Prism 5.0 and then were fitted by applying Boltzmann Sigmoid. The error bar represents SEM of the mean from three experiments.

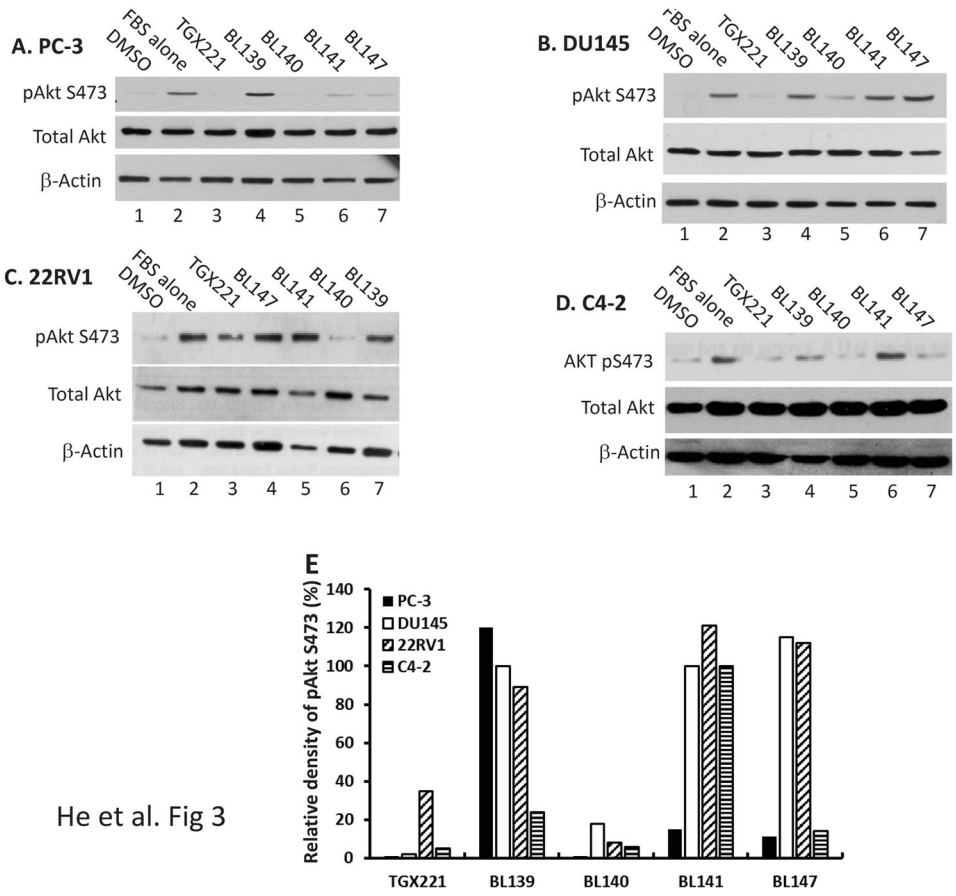

Fig 3.

TGX221 analogs inhibits AKT S473 phosphorylation. **A–D**. Prostate cancer cells (PC-3, DU145, 22RV1 and C4-2) were serum-starved overnight and then pre-treated with the solvent DMSO or the compounds as indicated at 5 μM for 30 min. Cells were then stimulated with FBS (10%) for 30 min. Cells were harvested and Western blot was done with anti-AKT (total and pS473) antibodies. Actin blot served as protein loading control. **E**. The relative band density of pAkt S473 after normalized against total Akt levels were summarized in panel E. Data are representative of three separate experiments.

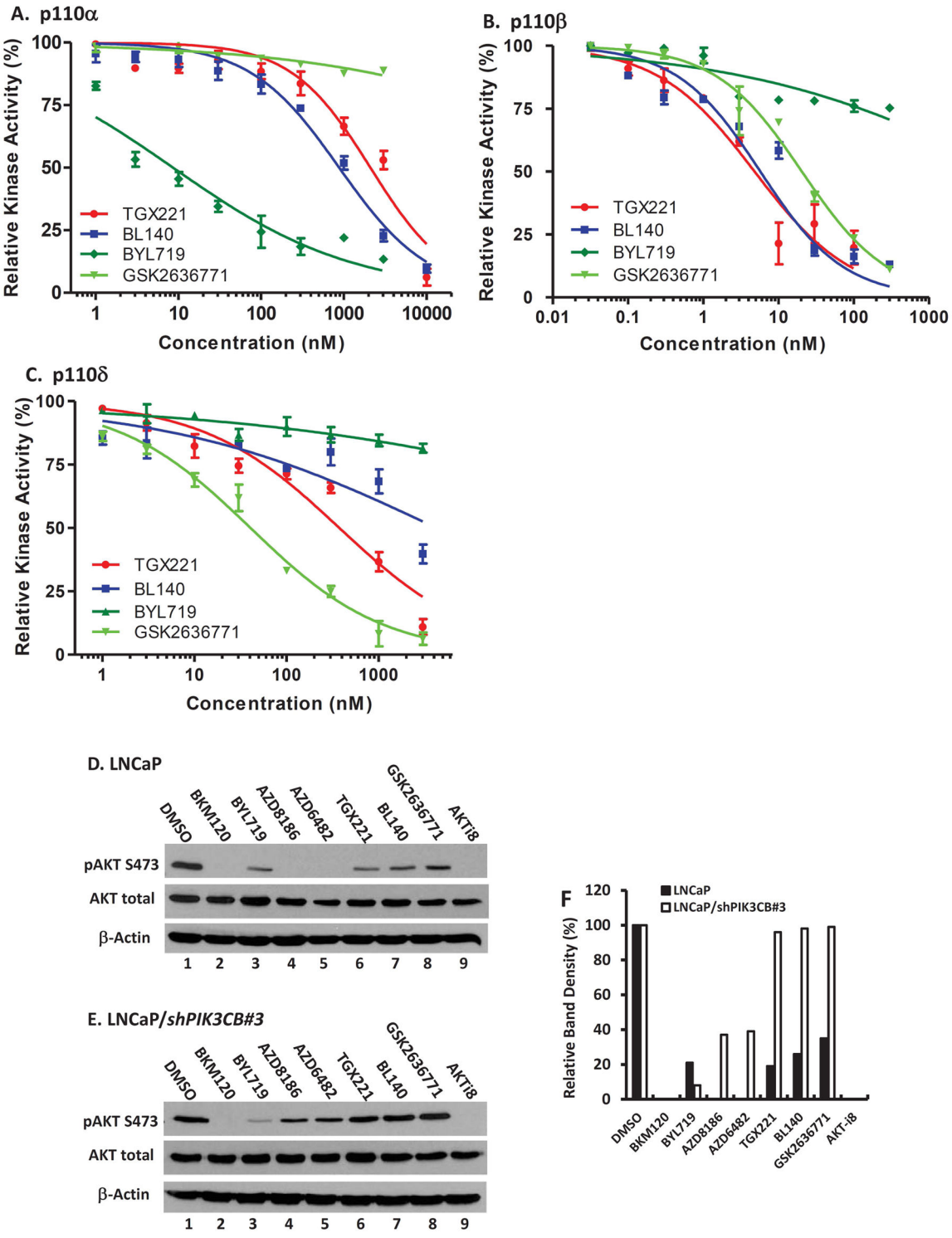

Fig 4.

PI3K isoform specificity. Kinase-Glo *in vitro* kinase assays were carried out in a 20 μl kinase buffer system (4 mM DTT, 2 μM ATP, 5 mM PIP2:PS) containing active complex of p110α/p85α (0.05 μg), p110β/p85α (0.3 μg) or p110δ/p85α (0.1 μg) in the presence of the

compound as indicated. Inhibition of individual kinase activity was calculated as a percentage reduction of luminescent signal in the presence of the compound compared to the solvent control (set as 100%). Data were plotted against the compound concentrations and curve fit was conducted using sigmoidal dose-response with variable slope (GraphPad Prism 5.0 software). Data were presented as MEAN ± SEM from three independent experiments. The parental LNCaP (**D**) and its PIK3CB silenced subline LNCaP/shPIK3CB#3 (**E**) were seeded in regular media and treated with the solvent or the compounds as indicated at 5 μM for 4 hrs. Cells were harvested and cellular protein lysates were subjected to Western blot with the antibodies as listed on the left side of each panel. **F**. The relative band density of pAkt S473 after normalized against total AKT compared to the DMSO control (set as 100%) was summarized and graphed. Data are representative of three separate experiments.

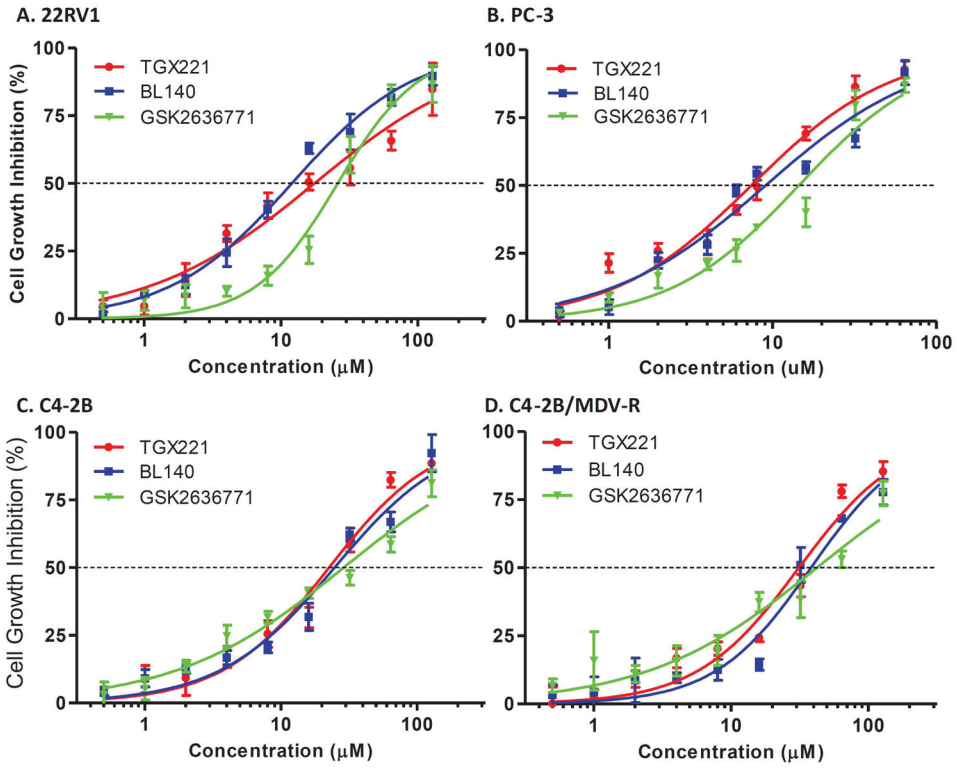

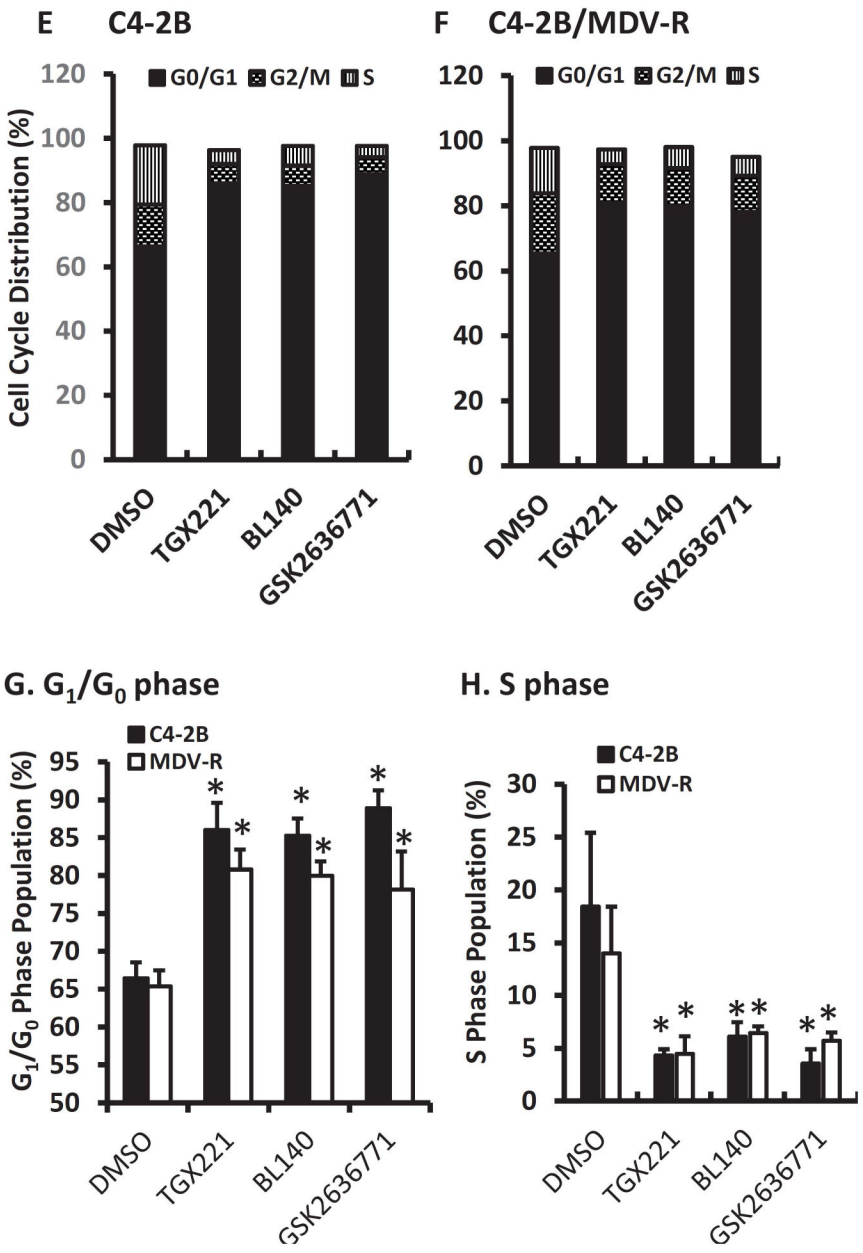

Fig 5.

Cell growth inhibition of CRPC cells. Prostate cancer 22RV1, PC-3, C4-2B and its MDV3100-ressitant subline (C4-2B/MDV-R) were seeded in 96-well plates and treated with the solvent or increasing concentrations of the compounds as indicated for three days. Cell growth was evaluated using WST-8 assay and the relative growth inhibition were calculated as a percentage value of the OD values at each treatment against the solvent control (set as 100%). Data from three independent experiments were plotted and the curve were fitted by applying compound concentration (log value) *vs.* normalized inhibitory response (percentage value) with variable slope (Graphpad Prism 5.0 software). C4-2B (**E**) and C4-2B/MDV-R (**F**) cells were serum-starved for overnight. After addition of the solvent or

the compounds for 30 min, cells were stimulated with 10% FBS for 16 h. Cells were harvested for flow cytometry analysis of cell cycle distribution with the propidium iodide-based protocol. Quantitative data of G_0/G_1 phase (**G**) and S phase (**H**) population were summarized from two independent experiments. The asterisk indicates a significant difference (Student t-test, $P < 0.05$) between the compound treatment and the solvent control.

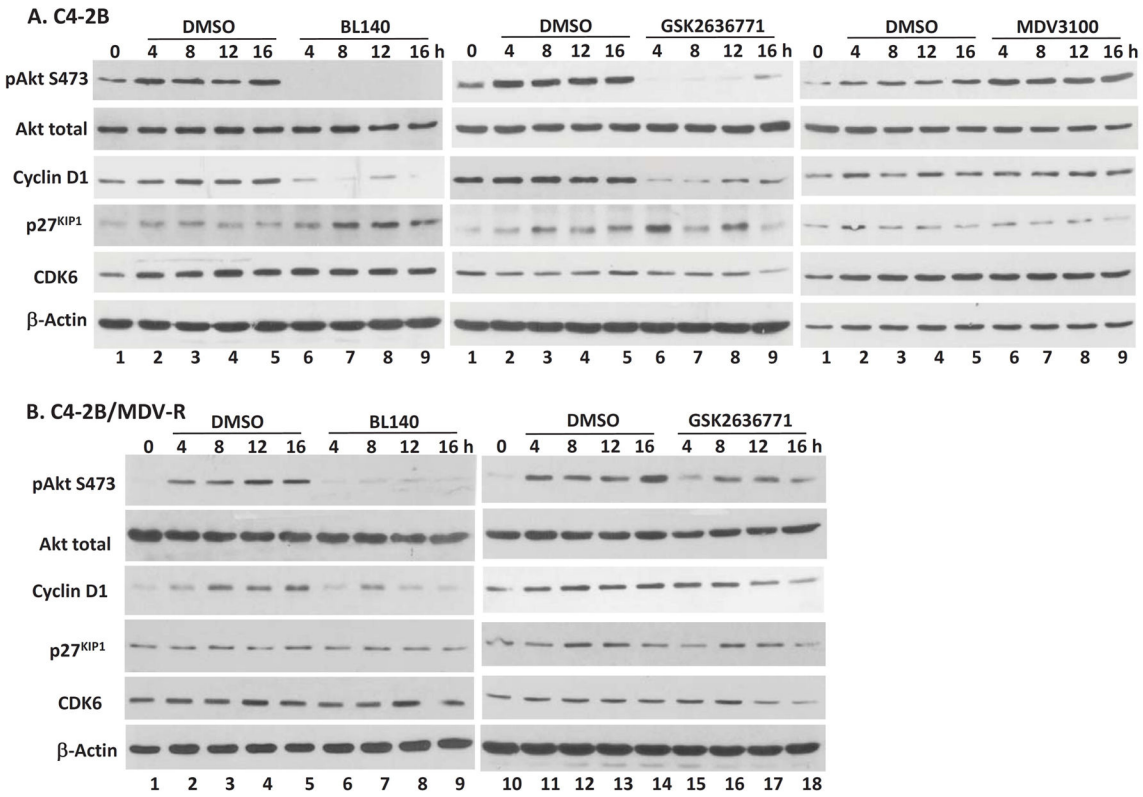

Fig 6.

PI3K/p110β inhibition reduces cyclin D1 but increases $p27^{kip1}$ protein levels. C4-2B (**A**) and C4-2B/MDV-R (**B**) cells were serum-starved for overnight. After a 30-min pretreatment with the solvent or the compounds (5 μM), cells were stimulated with 10% FBS and harvested at different time-points as indicated for Western blot with the antibodies listed on the left side of each panel. Actin blots served as protein loading control. Data were representative of two separate experiments.

Tab 1

Aqueous solubility of the TGX221 analogs.

Analog	M.W.	mg/ml	mM	ref.28
TGX221	364	< 1.0	<2.74	TGX-221
BL140	371	27.6	74.39	TGX-221a
BL141	371	36.8	99.19	TGX-221b
BL139	377	37.4	99.20	TGX-221c
BL138	384	31.6	84.17	TGX-221d
BL147	384	26.8	69.79	TGX-221e

Tab 2

The ΔT_m50 (°C) values are summarized for individual proteins from cell lysate (*in vitro*) and whole cell (*in vivo*) CETSA assays.

The ΔT_m50 (C) values for individual proteins *in vitro* and *in vivo*

	cell lysate (*in vitro*)					whole cell (*in vivo*)	
Compound	**p110α**	**p110β**	**p110γ**	**VPS34**	**Akt**	**p110β**	**Akt**
TGX221	1.57	**04.02**	0.68	0.42	1.49	1.72	1.18
BL139	1.51	**12.40**	0.84	0.14	2.44	**5.78**	2.60
BL140	1.16	**06.58**	1.73	0.55	2.14	**7.93**	3.14
BL141	1.61	**10.53**	0.61	0.84	0.52	1.32	2.31
BL147	1.47	03.83	1.43	**4.16**	1.45	2.18	2.85

Tab 3

IC_{50} values for the compounds towards individual PI3K isoform.

Class IA PI3K Kinase Assay (IC_{50} nM)

PI3K	TGX221	BL140	BYL719	GSK2636771
p110α	2091	878	8.619	3.54E+06
p110β	**4.813**	**5.744**	10402	**20.49**
p110δ	374	4247	5.92E+06	**40.53**

Tab 4

EC_{50} values from each compound in four cell lines tested were calculated using the data as presented in Fig 6.

Cell Growth Inhibition (WST-8 assay, EC_{50} μM)

	TGX221 (95% CI)	BL140 (95% CI)	GSK2636771 (95%CI)
C4-2B	22.61 (17.70–28.88)	24.79 (18.32–33.54)	28.93 (21.43–39.07)
C4-2B/MDV-R	31.29 (23.37–41.89)	38.28 (29.23–50.13)	42.26 (27.87–64.07)
22RV1	17.61 (12.75–22.33)	12.01 (10.32–13.99)	26.05 (20.97–32.36)
PC-3	07.43 (5.827–9.475)	9.077 (6.585–12.51)	14.48 (10.79–19.44)